Identification of a target protein of *Hydra* actinoporin-like toxin-1 (HALT-1) using GST affinity purification and SILAC-based quantitative proteomics

Type of paper: Original Research Article

Ameirika [a], Hong Xi, Sha [a], Jung Shan, Hwang [b, *]

[a] *Faculty of Applied Sciences, UCSI University, No.1, Jalan Menara Gading, UCSI Heights Cheras, 56000 Kuala Lumpur, Malaysia*

[b] *Sunway Institute for Healthcare Development, Sunway University, No.5 Jalan Universiti, Bandar Sunway, 47500 Selangor Darul Ehsan, Malaysia*

Ameirika's email: ameirika@gmail.com

Hong Xi, Sha's email: 2612326@live.cn

***Corresponding author**
Jung Shan, Hwang
Sunway Institute for Healthcare Development
Sunway University
No. 5, Jalan Universiti,
Bandar Sunway, 47500 Selangor Darul Ehsan
Malaysia
Tel: +603 7491 8622 (Ex. 7367)
Email: hwangjs@sunway.edu.my

Keywords:
actinoporin
cytolysin
folate receptor alpha
pore-forming protein
Hydra
protein-protein interactions

Abstract

Hydra actinoporin-like toxin-1 (HALT-1) is a 20.8 kDa pore-forming toxin isolated from *Hydra magnipapillata*. HALT-1 shares structural similarity with actinoporins, a family that is well known for its haemolytic and cytolytic activity. However, the precise pore-forming mechanism of HALT-1 remains an open question since little is known about the specific target binding for HALT-1. For this reason, a comprehensive proteomic analysis was performed using affinity purification and SILAC-based mass spectrometry to identify potential protein-protein interactions between mammalian HeLa cell surface proteins and HALT-1. A total of 4 mammalian proteins was identified, of which only folate receptor alpha was further verified by ELISA. Our preliminary results highlight an alternative-binding mode of HALT-1 to the human plasma membrane. This is the first evidence showing that HALT-1, an actinoporin-like protein, binds to a membrane protein, the folate receptor alpha. This study would advance our understanding of the molecular basis of toxicity of pore-forming toxins and provide new insights in the production of more potent inhibitors for the toxin-membrane receptor interactions.

1. Introduction

Pore-forming toxins (PFTs) are characterized by their unique ability to form pores in the cell membrane. They are produced by a variety of organisms such as bacteria (Geny and Popoff, 2006), yeast-fungi (Bussey, 1991) and human (Voskoboinik et al., 2010). In sea anemones, a group of alpha helical-pore-forming toxins (α-PFTs) was isolated and named actinoporins (Ferlan and Lebez, 1974; Kem, 1988; Turk, 1991). This group of toxins has characteristic features of PFTs, including small protein size of 18-20 kDa, an isoelectric point above 9, lack of cysteine residues and sphingomyelin dependence for membrane binding (Anderluh and Maček 2003; Norton 2009). The most studied members of the actinoporin family are equinatoxin II (EqtII) of *Actinia equina* and sticholysin II (StnII) of *Stichodactyla helianthus* (Šuput 2014; Rojko et al. 2016).

After the first actinoporin was identified in *Actinia equina*, many other actinoporin-like proteins were identified in other cnidarians. For example, six *Hydra* actinoporin-like toxins (HALTs) were identified in the genome of *Hydra magnipapillata* (Glasser et al. 2014). The amino acid sequences of these toxins share 30% identity with those of actinoporins from sea anemones (Glasser et al. 2014). In addition, HALT-1 showed haemolytic and cytolytic activity towards red blood cells and HeLa cells (Glasser et al. 2014; Liew et al. 2015). HALT-1 has a conserved cluster of aromatic amino acids and an amphiphilic N-terminus, which are proposed to play important roles in membrane binding and pore formation, respectively (Liew et al. 2015). Although HALT-1 is structurally similar to other actinoporins, a recent study showed that this toxin produced a different pore size from EqtII and did not use sphingomyelin as membrane target (Glasser et al. 2014). These findings may not be surprising, since HALT-1 and EqtII share only 30% similarity in protein sequence and several amino acid residues known to be involved in sphingomyelin binding in equinatoxin and sticholysin are not conserved in HALT-1 (Liew et al 2015).

Although numerous experiments support a critical role for sphingomyelin as the membrane attachment site for sea anemone antinoporins (Bakrač and Anderluh 2010), some reports suggested otherwise. For example, De los Ríos et al. (1998) and Caaveiro et al. (2001) tested the lytic action of StnII and EqtII with model membranes having different lipid compositions. Their results showed that these toxins appeared to have the ability to bind to and permeabilize membranes in the absence of sphingomyelin. In fact, EqtII was able to permeabilize large unilamellar vesicles (LUV) containing 30% cholesterol in egg phosphatidylcholine (Caaveiro et al. 2001) as well as LUVs composed of 1,2-dioleoyl-sn-glycero-3-phosphocholine (DOPC), 1,2-dipalmitoyl-sn-glyerol-3-phosphocholine (DPPC) and cholesterol (1:1:1) (Schön et al. 2008). A similar result was obtained with another actinoporin, sticholysin of *Stichodactyla helianthus*. This actinoporin was able to permeabilize LUVs composed only of cholesterol and phosphatidylcholine (De los Ríos et al. 1998; Anderluh and Maček 2003; Kristan et al. 2009). Thus, at least in some *in vitro* experiments, sphingomyelin is not required for membrane permeabilization by actinoporins.

In the present study, we have searched for alternative membrane receptors, in particular membrane proteins, which could play a role in HALT-1 permeabilization of membranes. The cell membrane is a complex mixture of lipids and proteins and both are functionally important in many cellular processes including as a barrier to separate the interior of the cell from its environment, to selectively transport substances across the membrane and to act as membrane-bound receptors or mediators of signal transduction (Fernandis and Wenk 2007). A few bacterial pore-forming toxins have been proven to bind proteinaceous receptors in addition of their affinity to membrane lipids (Dal Peraro and van der Goot 2016; DuMont and Torres 2014). These pore-forming toxins include the intermedilysin (ILY) of *Streptococcus intermedius* which recognises CD59, an GPI-anchored protein, as the membrane receptor although it has been classified as a cholesterol-dependent cytolysin (Giddings et al. 2004). Hence, membrane proteins can be potential candidates as receptors for HALT-1.

Since the attempt to show sphingomyelin as an important membrane target site for HALT-1 was not successful (Glasser et al 2014) and there has been no information on membrane protein binding, we used a combination of GST affinity purification and SILAC based quantitative mass spectrometry to identify potential membrane proteins that bind to HALT-1. This combination offered a powerful approach to identify complexes associated with signalling mechanisms (Ong and Mann 2006), including those involving low abundant proteins and weak protein interactions (Bauer and Kuster 2003). Using this approach we have identified a membrane protein, which appears to have a role in the binding of HALT-1 to membranes.

2. Materials and Methods

2.1. Plasmid construction

For the construction of glutathione-S-transferase-tagged (GST-tagged) at N-terminus of HALT-1 fusion protein, the Gateway cloning system (Invitrogen-Life Technologies, USA) was performed according to the manufacturer's instruction. Prior to the gene cloning, *HALT-1* was amplified from *HALT-1*-pCR4-TOPO using Phusion® High Fidelity DNA Polymerase (New England BioLabs, USA) and a pair of primers (forward primer 5'-CACCGCCAGTGGAGCAGCTTTAG-3' and reverse primer 5'-TTATCCAGAAAAAATAACTTTGAACTCAGCATGG-3'). The amplicon was then cloned into pENTR™/D-TOPO® Entry Vector using Directional TOPO cloning system to generate the Entry clone, and followed by the transformation into One Shot® TOP10 competent cells. To produce the expression vector containing GST-tagged at the N-terminus of HALT-1, the HALT-1 Entry clone was sub-cloned into pDEST™15 Destination vector using LR recombination reaction system and then transformed into Library Efficiency® DH5α cells. The construct of recombinant GST-tagged HALT-1 was finally verified by sequencing.

2.2. Protein expression and purification

The recombinant GST-tagged HALT-1 was expressed in BL21-AI™ One Shot® *E. coli* with L-(+)-arabinose induction (0.2%) for 4 hours at 30°C. After the expression, the cells were harvested by centrifugation at 10,000 xg for 5 min. Subsequently, the arabinose-induced culture was re-suspended in equilibration buffer (50 mM Tris.HCl, 150 mM NaCl, pH 8.0) with additional protease inhibitor PMSF (0.1 mM), and the cells were lysed by sonication at 500 watts and 20 kHz. The lysate was centrifuged 2,200 xg for 15 min. For protein purification, a total of 50-200 mg soluble fraction of cell lysate were subjected to affinity chromatography of glutathione agarose (Thermo Fisher Scientific, USA). Purified GST-tagged HALT-1 fusion

protein was concentrated and exchanged buffer with BupH Tris buffer using Amicon® Ultra-2 (Merck Millipore, USA). As based on the manufacturer's protocol of Quick Start Bradford Assay (Bio-Rad, USA), the final concentration of purified GST-tagged HALT-1 protein was measured as 10.8 μg/μL.

2.3. Cell culture and SILAC labelling

HeLa cells (ATCC® CCL-2™) were routinely maintained in Dulbecco's modified Eagle's medium (Gibco/Invitrogen-Life Technologies, USA) supplemented with 10% dialyzed fetal bovine serum (FBS) and 1% penicillin-streptomycin at 37°C in 5% CO_2 atmosphere. For SILAC labelling, the incorporation of "light" and "heavy" amino acids into cells was carried out using SILAC Protein Identification (ID) and Quantitation Kits (Gibco/Invitrogen-Life Technologies, USA) according to the manufacturer's instruction. Two sets of HeLa cells were grown separately in two different custom-made SILAC media, in which one group of cells was grown in normal or "light" medium containing 100 mg/mL of L-lysine HCl and 100 mg/mL of L-Arginine and the other group of cells was grown in labelling or "heavy" medium containing 100 mg/ mL of [U-$^{13}C_6$]-L-Lysine HCl (*Lys) and 100 mg/mL of L-Arginine. Both "light" and "heavy" media were supplemented with 4,500 mg/L of glucose, 292 mg/L of L-glutamine, 110 mg/L of sodium pyruvate, 15 mg/mL of phenol red, 1% of penicillin-streptomycin and 10% dialyzed FBS. "Light" and "heavy" labelled cell populations were passaged for at least 9 doubling times to achieve complete incorporation of [U-$^{13}C_6$]-L-Lysine HCl (*Lys) (Ong et al. 2002, 2003; Ong and Mann 2006). Both cell cultures were grown at 37°C in a humidified incubator of 5% CO_2 atmosphere. After cell adaptation, the efficiency of SILAC incorporation into the culture was determined to be >95% by mass spectrometry analysis. The percentage of SILAC incorporation was calculated manually using the following equation: Incorporation (%) = [Ratio (H/L) / (Ratio (H/L) + 1)] x 100 (Oeljeklaus et al. 2014).

2.4. Preparation of cell lysates

For sample preparation, both "light" and "heavy" labelled HeLa cell populations were separately grown to approximately 90% confluence in their respective SILAC media as described above. After that, the medium was removed and cells were washed with 0.9% sterile NaCl, scrapped in 0.9% sterile NaCl and centrifuged at 200 xg for 5 min at 4°C. Whole cell extracts were prepared by dissolving cells in Pierce IP lysis buffer (Thermo Fisher Scientific, USA) (25 mM Tris.HCl pH 7.4, 150 mM NaCl, 1% NP-40, 1 mM EDTA and 5% glycerol) with addition Halt™ Protease Inhibitor Single-Use Cocktail (Thermo Fisher Scientific, USA). Two cell suspensions were incubated for 7 min on ice with maximum agitation and subsequently pelleted with centrifugation at 13,000 xg for 10 min at 4°C. Supernatants of "light" and "heavy" labelled cell suspensions were ready for the GST affinity purification.

2.5. Affinity purification of GST-tagged HALT-1 binding proteins

To identify HALT-1 binding proteins in cell lysates we used a recombinant GST-HALT-1 fusion protein bound to glutathione agarose beads. Briefly, a total of 12 mg HeLa lysate from SILAC "heavy" medium was incubated with the GST-tagged HALT-1 protein (300 µg) immobilized on agarose beads for 30 min at 4°C. After washing nonspecific proteins from the column, the SILAC-labelled HeLa proteins that bound to HALT-1 were eluted with 2 mL of elution buffer (50 mM Tris.HCl, 150 mM NaCl, 10 mM reduced glutathione, pH 3.0). As a control for non-specific binding, an equal protein amount (12 mg) of HeLa lysate from the SILAC "light" medium was incubated with glutathione agarose beads only, followed by washing and elution. To replicate the experiment, the entire procedure was repeated with the "heavy" and "light" SILAC labels reversed. The HeLa cell lysate from "light" medium was incubated with the GST-HALT-1 fusion protein immobilized on glutathione agarose beads, whereas the HeLa cell lysate from "heavy" medium was incubated with glutathione agarose beads alone.

Equal amount of eluted proteins from “heavy” and “light” cell lysates were analysed in 12% sodium dodedyl suphate-polyacrylamide gel electrophoresis (SDS-PAGE) followed by zinc staining and mass spectrometry analyses.

2.6. Liquid chromatography-tandem mass spectrometry and data analysis

Pooled proteins obtained from the affinity purification were incorporated into a polyacrylamide gel matrix to form a tube-gel (Lu and Zhu 2005) and sent to the Protein and Proteomic Centre, National University of Singapore for the liquid chromatography–tandem mass spectrometry (LC-MS/MS). In brief, the polyacrylamide gel was excised and further processed to in-gel reduction, alkylation, trypsin in-gel digestion and sample desalting/clean up according to the standard in-gel digestion protocol as described previously with minor modifications (Fukada et al. 2004; Lu and Zhu 2005). The finely cut gels were washed with 25 mM ammonium bicarbonate (AMBIC) and dehydrated with 100% acetonitrile (ACN). Subsequently, the samples were reduced with 10 mM dithiothreitol (DTT) for 30 min at 60°C, followed by alkylation with 55 mM iodoacetamide (IAA) for 30 min at room temperature in the dark. The gel pieces were then washed with 25 mM AMBIC, dehydrated with ACN and dried using vacuum centrifuge. After that, the samples were incubated overnight at 37°C with 10 ng/μL trypsin in 25 mM AMBIC for proteolytic digestion of proteins. On the following day, the peptides were extracted from the gel using 50 μL of 25 mM AMBIC, 100 μL of 0.02% heptafluorobutyric acid (HFBA) in deionised water, 150 μL of 0.02% HFBA in 50% ACN and 50 μL of 100% ACN. Hence, four different supernatant fractions from the peptides extraction steps were subsequently pooled together, lyophilized using vacuum centrifuge and desalted prior subjected to LC-MS/MS. Separation of peptides from tryptic peptide mixture was carried out using Eksigent Nano-liquid chromatography (AB SCIEX, USA) for 100 minutes, followed by the MS analysis using Triple TOF 5600 system (AB SCIEX, USA). To identify the proteins, the mass spectra acquired from the mass spectrometry were searched against the human and decoy (reversed) databases using a Paragon™ Algorithm (Shilov et al. 2007), ProteinPilot software package version 4.5 (AB

SCIEX, USA). The target-decoy approach was set at 5% of false discovery rate (FDR) (Choi and Nesvizhskii 2008; Elias and Gygi 2010).

2.7. Statistical data analysis

The data files acquired from LC-MS/MS were viewed and further processed with ProteinPilot version 4.5 software. Here, the data were normalized using global median normalization that shifted the centre of the distribution to zero without affecting the spread. For protein identification and quantitation, only proteins with minimum of 2 unique peptides and proteins that were identified in the experimental replicates with 95% confidence were considered as the candidate protein interactors. In addition, the fold-change approach (SILAC (H/L) $\geq$ 2.0 fold) was applied to identify protein interaction partners and hence, identified proteins with low fold-change value from the threshold were discarded. The protein SILAC ratio and its intensity values were inverted for the "reversed" experiment mentioned in 2.5 of this section.

For statistical analysis, Student's t-test (paired sample) followed by the multiple testing Benjamini-Hochberg correction was used to obtain the statistical significance value (p-value < 0.05) (Benjamini and Hochberg 1995), using the Statistical Package for the Social Sciences (SPSS) software, version 23.

2.8. Bioinformatics analysis

The information of subcellular localization, molecular function and biological process of the identified proteins were obtained from Gene Ontology (GO) (http://geneontology.org) (Ashburner et al. 2000; The Gene Ontology Consortium 2015) and UniProt (http://www.uniprot.org) (The UniProt Consortium 2017).

2.9. Enzyme linked immunosorbent assay (ELISA)

19.69 nM of human recombinant folate receptor alpha (FOLR-1, Sigma-Aldrich, USA) was immobilized on the immunoplate (SPL 96-well immunoplate, SPL Sciences Co., Ltd.,

Korea) overnight at 4°C. On the next day, the wells were emptied and washed 3 times with 150 µL of PBST buffer (PBS with 0.2% of Tween-20) for 5 min each. The unoccupied protein-binding sites in wells were blocked by adding 200 µL of 1% BSA in PBS buffer (pH 7.4) and further incubation at room temperature for 2 hours. After a routine washing process, 100 µL of HALT-1 (20, 40, 80, 160, 320 and 400 nM) were added to the wells and incubated for 2 hours at room temperature. The wells were rinsed three times with PBST buffer before incubating with 100 µL of rabbit α-HALT-1 antibody (1:2000). Then, 100 µL of goat α-rabbit IgG-AP (1:8000) (Santa Cruz Biotechnology, USA) were added and incubated at room temperature for 2 hours. After three rinses, 50 µL of substrate 4-MUP (4-methylumbelliferyl-phosphate, Sigma-Aldrich, USA) was added to each well to develop the fluorescent signal. Measurement of the fluorescent signal (excitation/emission at 355/460 nm) was performed by a multi-mode microplate reader (BMG Labtech, Germany). The intra-assay variability was calculated from the average of triplicate wells in one microplate.

3. Results and Discussion

3.1 Identification of potential HALT-1 interaction partners

To identify HALT-1-interacting proteins that could mediate HALT-1 membrane binding, we performed a comprehensive proteomic analysis using SILAC-based quantitative affinity purification and mass spectrometry (SILAC-based q-AP-MS). The schematic workflow of this experiment is presented in Fig.1 including SILAC labelling, affinity purification (by GST pull-down) and LC-MS/MS. The SILAC procedure was used to distinguish protein(s) binding to HALT-1 from nonspecific proteins binding to the glutathione matrix. We first tested the efficiency of SILAC incorporation in HeLa cells after 9 doubling times in SILAC media and its influence on the accuracy and reliability of quantitative mass spectrometry. For this experiment, only heavy labelled HeLa cells were prepared and subsequently processed for protein quantification by LC-MS/MS. The result showed a SILAC-labelling efficiency of 97.33% in HeLa cells, indicating that nearly all peptides or proteins were labelled with SILAC lysine residue (Supplementary Fig. S1). This level of SILAC labelling in HeLa cells was considered satisfactory, since it fell within the range (95-97%) reported in other SILAC labelling experiments (Zhu et al. 2002; Waanders et al. 2007).

To identify potential HALT-1 interacting proteins a “heavy” cell lysate was added to a column containing GST-tagged HALT-1 immobilized on glutathione agarose beads while a “light” cell lysate was added to a column containing only glutathione agarose beads. In a second experiment, the labels were reversed: the “light” cell lysate was added to GST-tagged HALT-1 immobilized on glutathione agarose beads and the “heavy” cell lysate was added to the column containing glutathione agarose alone. Two pools of proteins collected separately from the eluate fractions of two individual experiments described above were examined by 12% SDS-PAGE gel electrophoresis under reducing condition and then visualized by zinc stain (Supplementary Fig. S2) before they were combined for LC-MS/MS analysis. Data of LC-MS/MS were analysed

against the human and decoy (reversed sequences) database using Paragom™ Algorithm, ProteinPilot software package (version 4.5, AB SCIEX, USA). In brief, a total of 2,458 and 1,752 tandem mass spectra were generated from the two experimental replicates, respectively. Subsequently these two numbers resulted in 105 and 117 unique proteins. By using ProteinPilot, we normalized the mass spectrometry data result with global median normalization with aims to minimize the variation between the two data sets. Subsequently, we carried out the quantitation analysis for each peptide and removed proteins which did not have at least 2 unique peptide hits at 5% FDR (False Discovery Rate). As a result, lists comprising of 41 and 32 protein hits were generated and compiled in tables 1 and 2, respectively. Instead of a direct calculation of "heavy" (H) over "light" (L) ratio, ProteinPilot used correction algorithm to measure the percentage error due to various experimental bias. These proteins varied in their SILAC (H/L) ratios and were localized in various subcellular compartments as determined by the Gene Ontology.

To further strengthen the selection of interaction partners for HALT-1, only proteins with SILAC (H/L) ratios ≥2.0 with significant confidence level at 95% (p-value < 0.05) were considered as possible interaction partners for HALT-1. These putative interaction partners of HALT-1 have to be present in both tables 1 and 2, and they include 60S ribosomal protein L12, 60S acidic ribosomal protein P2, folate receptor alpha and nucleolin (Table 3). Figure 2 demonstrated that the intensities of "light" and "heavy" labelled peptides differ by at least 2.0 fold in the MS/MS spectra for each putative HALT-1 interactor (Fig. 2). Of the four putative HALT-1 interactors, we eliminated nucleolin, 60S ribosomal protein L12, and 60S acidic ribosomal protein P2 as nonspecific binding partners, since they are abundant intracellular proteins and are known to interact with affinity matrices such as sepharose (Gingras et al. 2007; Trinkle-Mulcahy et al. 2008). Furthermore, they are commonly detected protein contaminants in q-AP-MS experiments (Oeljeklaus et al. 2009). Therefore, we focused our attention on one candidate, folate receptor alpha, which gave a strong H/L signal in both experiments and is located on the cell membrane and thus a potential target for HALT-1.

3.2 Verification of folate receptor alpha binding to HALT-1

To verify the interaction between HALT-1 and folate receptor alpha, we performed an ELISA binding assay with various HALT-1 concentrations to folate receptor alpha that was coated on the well surface of immunoplate. Figure 3 shows that HALT-1 bound to folate receptor alpha in a dose-dependent manner ranging from 0 to 400 nM (or 0 to 10 μg/mL). The intensity of signal has not reached a plateau because the amount of HALT-1 has yet to saturate the coated FOLR1 but the antibodies used was enough to give a discernible detection signal at the highest concentration of HALT-1. Controls lacking either folate receptor alpha, HALT-1, anti-HALT-1 antibody or secondary antibody resulted in very low or insignificant signals. Therefore, there was a direct, *in vitro* binding of HALT-1 to folate receptor alpha suggesting a possible involvement of folate receptor alpha in the mechanism of HALT-1 induced cell lysis.

3.3 Concluding remarks

The folate receptor alpha is a GPI-anchored (glycosylphosphatidylinositol-anchored) membrane protein of 38-40 kDa that plays a major role in the uptake of folate/folic acid into cells via endocytosis (Luhrs and Slomiany 1989; Basal et al. 2009). Folate receptor alpha is attached to the GPI anchor via its C-terminal end (Paulick and Bertozzi 2008; Maeda and Kinoshita 2011). Therefore, the folate receptor alpha is localized on the outer surface of the cell membrane and could serve as the membrane attachment site for extracellular proteins, possibly including HALT-1. This hypothesis is supported by the fact that the alpha-toxin of *Clostridium septicum* binds to the GPI-anchored form of folate receptor alpha (Gordon et al. 1999) before it is cleaved approximately 4 kDa from the C-terminus to become an active cytolysin (Melton-Witt et al. 2006). Similarly, we suggest that folate receptor alpha could serve as a membrane receptor for HALT-1 instead of the lipid sphingomyelin, which has been previously thought to be the solely attachment site for HALT-1 on the cell membrane (Liew et al. 2015). This idea is

supported by the results of Glasser et al. (2014) who pointed out the likelihood of an alternative binding site for HALT-1. In brief, these authors compared the binding affinity of sphingomyelin to HALT-1 and EqtII in a haemolysis assay. Their results clearly showed that the concentration of sphingomyelin that fully inhibited the haemolytic activity of EqtII failed to block the haemolytic activity of HALT-1. Thus, the binding affinity of HALT-1 to sphingomyelin is at least 100-fold weaker than that of EqtII. HALT-1 also lacks conserved amino acids in the sphingomyelin binding site.

We cannot totally rule out the possibility that HALT-1 binds to more than one attachment sites on cell membrane since some bacterial pore-forming toxins are able to bind more than one membrane receptors. A good example is the intermedilysin (ILY) of *Streptococcus intermedius* which recognises CD59, an GPI-anchored protein, as the membrane receptor although it has been classified as a cholesterol-dependent cytolysin (Giddings et al. 2004). α-hemolysin of *Staphylococcus aureus* is another example of PFTs binding to multiple membrane target sites. α-hemolysin has been known to have a low affinity to phosphocholine head groups but it was later proven to interact with ADAM10 (a disintegrin and metalloprotease 10) which is a transmembrane protease present in wide variety of cells (Valeva et al. 2006; Wilke and Wardenburg 2010).

In summary, by a combination of affinity purification and SILAC-based quantitative mass spectrometry we have identified the folate receptor alpha as an interaction partner of HALT-1. This result provides an alternative to the previously established binding of HALT-1 to the lipid sphingomyelin. By identifying the potential membrane receptors for HALT-1, we have unravelled the essential step in the lytic mechanism by *Hydra*'s toxin. The next step is to gain a deeper understanding of the possible role of folate receptor alpha in pore formation. This is particularly crucial to understand how the initial toxin-membrane receptor interaction leads to the subsequent adverse effects or illness in host body. The findings of this study also provided a broad implication for making anti-PFTs therapies that aims to disrupt the toxin-membrane

receptor interactions. For most toxins, their interactions with membrane receptors are highly specific and hence the therapies can target these specific interactions and leave other receptor sites unharmed.

Conflict of interest

The authors affirm that they have no conflict of interest to report their work.

Acknowledgements

We would like to express our sincere thanks to Prof. Charles N. David (Ludwig-Maximilians-Universität München, Germany) for his critical reading of the manuscript and giving constructive suggestions for improvement. Our gratitude also extends to Assistant Professor Dr. Lin Qing Song and his team (Protein and Proteomics Centre, National University of Singapore) for technical support and analytical assistance in quantitative shotgun mass spectrometry. This work was generously supported by the Fundamental Research Grant Scheme, Ministry of Higher Education Malaysia (Grant No. FRGS/1/2013/ST03/UCSI/02/1).

References

Anderluh, G., Maček, P., 2003. Actinoporins, pore-forming toxins of sea anemones (Actinaria), in: Menestrina, G., Dalla, S.M., Lazarovici, M (Eds.), Pore-forming peptides and protein toxins. Taylor and Francis Press, London, pp. 132-147.

Ashburner, M., Ball, C.A., Blake, J.A., Botstein, D., Butler, H., Cherry, M., Davis, A.P., Dolinski, K., Dwight, S.S., Eppig, J.T., Harris, M.A., Hill, D.P., Issel-Tarver, L., Kasarskis, A., Lewis, S., Matese, J.C., Richardson, J.E., Ringwald, M., Rubin, G.M., Sherlock, G., 2000. Gene Ontology: tool for the unification of biology. Nat. Genet. 25, 25-29.

Bakrač, B. Anderluh, G., 2010. Molecular mechanism of sphingomyelin-specific membrane binding and pore formation by actinoporins. Adv. Exp. Med. Biol. 677, 106-115.

Basal. E., Eghbali-Fatourechi, G.Z., Kalli, K.R., Hartmann, L.C., Goodman, K.M., Goode, E.L., Kamen, B.A., Low, P.S., Knutson, K.L., 2009. Functional folate receptor alpha is elevated in the blood of ovarian cancer patients. PLoS One 4, e6292.

Bauer, A., Kuster, B., 2003. Affinity purification-mass spectrometry. Powerful tools for the characterization of protein complexes. Eur. J. Biochem. 270, 570-578.

Benjamini, Y., Hochberg, Y., 1995. Controlling the false discovery rate: a practical and powerful approach to multiple testing. J. Royal Stat. Soc. 57, 289-300.

Bussey, H., 1991. K1 killer toxin, a pore-forming protein from yeast. Mol. Microbiol. 5, 2339-2343.

Caaveiro, J.M.M., Echabe, I., Gutiérrez-Aguirre, I., Nieva, J.L., Arrondo, J.L.R., Gonzălez-Mañas, J.M., 2001. Differential interaction of equinatoxin II with model membranes in response to lipid composition. Biophys. J. 89, 1343-1353.

Choi, H., Nesvizhskii, A.I., 2008. False discovery rates and related statistical concepts in mass spectrometry-based proteomics. J. Proteome Res. 7, 47-50.

Dal Peraro, M., van der Goot, F.G., 2016. Pore-forming toxins: ancient, but never really out of fashion. Nat. Rev. Microbiol. 14, 77-92.

De los Ríos, V., Mancheno, J.M., Lanio, M.E., Onaderra, M., Gavilanes, J.G., 1998. Mechanism of the leakage induced on lipid model membranes by the haemolytic protein sticholysin II from the sea anemone *Stichodactyla helianthus*. FEBS J. 252, 284-289.

DuMont, A.L., Torres, V.J., 2014. Cell targeting by the *Staphylococcus aureus* pore-forming toxins: it's not just about lipids. Trends in Microbiol. 22, 21-27.

Elias, J.E., Gygi, S.P., 2010. Target-decoy search strategy for mass spectrometry-based proteomics. Methods Mol. Biol. 604, 55-71.

Ferlan, I., Lebez, D., 1974. Equinatoxin, a lethal protein from *Actinia-equina*-I, purification and characterization. Toxicon 12, 57-61.

Fernandis, A.Z., Wenk, M.R., 2007. Membrane lipids as signalling molecules. Curr. Opin. Lipidol. 18, 121-128.

Fukada, K., Zhang, F., Vien, A., Cashman, N.R., Zhu, H., 2004. Mitochondrial proteomic analysis of a cell line model of familial amyotrophic lateral sclerosis. Mol. Cell Proteomics 3, 1211-1223.

Geny, B., Popoff, M.R., 2006. Bacterial protein toxins and lipids: pore formation of toxin entry into cells. Biol. Cell 98, 667-678.

Giddings, K.S., Zhao, J., Sims, P.J., Tweten, R.K., 2004. Human CD59 is a receptor for the cholesterol-dependent cytolysin intermedilysin. Nat. Struct. Mol. Biol. 11, 1173–1178.

Gingras, A.C., Gstaiger, M., Raught, B., Aebersold, R., 2007. Analysis of protein complexes using mass spectrometry. Nature Rev. Mol. Cell Biol. 8, 645-654.

Glasser, E., Rachamim, T., Aharonovich, D., Sher, D., 2014. *Hydra* actinoporin-like toxin-1, an unusual hemolysin from the nematocyst venom of *Hydra magnipapillata,* which belongs to an extended gene family. Toxicon 91, 103-113.

Gordon, V.M., Nelson, K.L., Buckey, J.T., Stevens, V.L., Tweten, R.K., Elwood, P.C., Leppla, S.H., 1999. *Clostridium septicum* alpha toxin uses glycosylphosphatidylnositol-anchored protein receptors. J. Biol. Chem. 274, 27274-27280.

Kem, W.R., 1988. Sea anemone toxins: structure and action, in: Hessinger, D.A., Lenhoff, H.M. (Eds.), The Biology of Nematocyst. Academic Press, San Diego, pp 375-405.

Kristan, K. Č. Viero, G., Serra, M.D., Maček, P., Anderluh, G., 2009. Molecular mechanism of pore formation by actinoporins. Toxicon 54, 1125-1134.

Liew, Y.J.M., Soh, W.T., Jiemy, W.F., and Hwang, J.S., 2015. Mutagenesis and functional analysis of the pore-forming toxin HALT-1 from *Hydra magnipapillata*. Toxins 7, 407-422.

Lu, X., Zhu, H., 2005. Tube-gel digestion: a novel proteomic approach for high throughput analysis of membrane protein. Mol. Cell. Proteomics 4, 1948-1958.

Luhrs, C.A., Slomiany, B.L., 1989. A human membrane-associated folate binding protein is anchored by a glycosyl-phosphathidylinositol tail. J. Biol. Chem. 264, 21445-21449.

Maeda, Y., Kinoshita, T., 2011. Structural remodelling, trafficking and functions of glycosylphosphatidylinositol-anchored proteins. Prog. Lipid Res. 50, 411-424.

Melton-Witt, J.A., Bentsen, L.M., Tweten, R.K., 2006. Identification of functional domains of *Clostridium septicum* alpha toxin. Biochemistry 45, 14347-14354.

Norton, R.S., 2009. Structures of sea anemone toxins. Toxicon 54, 1075-1088.

Oeljeklaus, S, Schummer, A., Suppanz, I., Warscheid, B., 2014. SILAC labelling of yeast for the study of membrane protein complexes, in: Warscheid, B. (Eds.), Stable isotope labelling by amino acids (SILAC): Methods and Protocols. Springer, New York, pp 23-46.

Oeljeklaus, S., Mayer, H.E., Warscheid, B., 2009. New dimensions in the study of protein complexes using quantitative mass spectrometry. FEBS Lett. 583, 1674-1683.

Ong, S.E., Blagoev, B., Kratchmarova, I., Kristensen, D.B., Steen, H., Pandey, A., and Mann, M., 2002. Stable isotope labeling by amino acids in cell culture, SILAC, as a simple and accurate approach to expression proteomics. Mol. Cell. Proteomics 1, 376-386.

Ong, S.E., Kratchmarova, I., Mann, M., 2003. Properties of ^{13}C-substituted arginine in stable isotope labelling by amino acids in cell culture (SILAC). J. Proteome Res. 2, 173-181.

Ong, S.E., Mann, M., 2006. A practical recipe for stable isotope labeling by amino acids in cell culture (SILAC). Nat. Protoc. 1, 2650-2660.

Paulick, M.G., Bertozzi, C.R., 2008. The glycosylphosphatidylinositol anchor: A complex membrane-anchoring structure for proteins. Biochemistry 47, 6991-7000.

Rojko, N., Dalla Serra, M., Maček, P., Anderluh, G., 2016. Pore formation by actinoporins, cytolysins from sea anemones. Biochimica et Biophysica Acta (BBA)-Biomembranes 1858, 446-456.

Schön, P., García-Sáez, A.J., Malovrh, P., Bacia, K., Anderluh, G., Schwille, P., 2008. Equinatoxin II permeabilizing activity depends on the presence of sphingomyelin and lipid phase coexistence. Biophys. J. 95, 691-698.

Shilov, I.V., Seymour, S.L., Patel, A.A., Loboda, A., Tang, W.H., Keating, S.P., Hunter, C.L., Nuwaysir, L.M., Schaeffer, D.A., 2007. The Paragon algorithm, a next generation search engine that uses sequence temperature values and feature

probability to identify peptides from tandem mass spectra. Mol. Cell. Proteomics 6, 1638-1655.

Šuput, D., 2014. Equinatoxins: A review, in: P. Gopalakrishnakone (Eds.), Marine and Freshwater Toxins, Springer Netherlands, Dordrecht, pp. 1–17.

The Gene Ontology Consortium, 2015. Gene Ontology Consortium: going forward. Nucleic Acids Res 43, D1049–D1056.

The UniProt Consortium, 2017. UniProt: the universal protein knowledgebase. Nucleic Acids Res. 45(D1), D158-D169.

Trinkle-Mulcahy, L., Boulon, S., Lam, Y.W., Urcia, R., Boisvert, F.M., Vandermoere, F., Morrice, N.A., Swift, S., Rothbauer, U., Leonhardt, H., Lamond, A., 2008. Identifying specific protein interaction partners using quantitative mass spectrometry and bead proteomes. J. Cell Biol. 183, 223-239.

Turk, T., 1991. Cytolytic toxins from sea anemones. J. Toxicol. 10, 223-262.

Valeva, A., Hellmann, N., Walev, I., Strand, D., Plate, M., Boukhallouk, F., Brack, A., Hanada, K., Decker, H., Bhakdi, S., 2006. Evidence that clustered phosphocholine head groups serve as sites for binding and assembly of an oligomeric protein pore. J. Biol. Chem. 281, 26014–26021.

Voskoboinik, I., Dunstone, M.A., Baran, K., Whisstock, J.C., Trapani, J.A., 2010. Perforin: structure, function, and role in human immunopathology. Immunol. Rev. 235, 35-54.

Waanders, L.F., Hanke, S., Mann, M., 2007. Top-down quantitation and characterization of SILAC-labelled proteins. J. Am. Soc. Mass Spectrum. 18, 2058-2065.

Wilke, G.A., Wardenburg, J.B., 2010. Role of a disintegrin and metalloprotease 10 in *Staphylococcus aureus* α-hemolysin–mediated cellular injury. PNAS USA. 107, 13473–13478.

Zhu, H., Pan, S., Gu, S., Bradbury, E. M., Chen, X., 2002. Amino acid residue specific stable isotope labelling for quantitative proteomics. Rapid Commun. Mass Spectrom. 16, 2115-2123.

TABLE 1 List of "heavy" labelled proteins interacting to HALT-1 in GST affinity purification

Accession number[a]	Protein name	Subcellular location	Molecular weight (kDa)	Intensity L	Intensity H	Ratio H/L[b]	Number of unique peptides[c]
P30050	60S ribosomal protein L12	Cytoplasm, cytosol, nucleus, nucleolus	17.819	0	428.29	100	5
Q9HAV7	GrpE protein homolog 1, mitochondrial	Mitochondrion matrix, nucleus	24.279	2.74	154.31	24.75	2
P04899	Guanine nucleotide-binding protein G(i) subunit alpha-2	Cytoplasm, cell membrane	40.451	11.27	107.29	6.93	2
P05387	60S acidic ribosomal protein P2	Cytosol, cell membrane	11.665	116.93	1690.2	6.35	11
Q12905	Interleukin enhancer-binding factor 2	Nucleus, cytoplasm	43.062	21.04	252.25	5.27	2
P19338	Nucleolin	Nucleus, cytoplasm, cell membrane	76.614	49.86	646.02	5.20	17
P15328	Folate receptor alpha	Cell membrane	29.819	81.51	895.81	4.83	4
P05386	60S acidic ribosomal protein P1	Cytoplasm, cytosol	11.514	43.43	473.75	4.79	2
P25398	40S ribosomal protein S12	Cytoplasm, cytosol	14.515	35	299.37	3.78	6
P08174	Complement decay-accelerating factor	Cell membrane	41.400	39.07	202.53	3.68	5
P53999	Activated RNA polymerase II transcriptional coactivator p15	Nucleus	14.395	21.88	120.46	2.42	2
P05186	Alkaline phosphatase, tissue-nonspecific isozyme	Cell membrane	57.305	23.74	123.86	2.29	2
P05388	60S acidic ribosomal protein P0-like; 60S acidic ribosomal protein P0	Cytosolic large ribosomal subunit, preribosome, large subunit precursor; Nucleus, cytoplasm	34.274	41.4	195.91	2.01	5
P60660	Myosin light polypeptide 6	Cytosol, membrane	16.930	109.17	458.44	1.81	11
Q9NYL9	Tropomodulin-3	Cytoplasm, cytoskeleton	39.595	29.26	110.525	1.72	2
P11021	78 kDa glucose-regulated protein	Endoplasmic reticulum lumen, melanosome, cytoplasm	72.333	41.985	158.80	1.72	4

TABLE 1 List of "heavy" labelled proteins interacting to HALT-1 in GST affinity purification (continue)

Accession number[a]	Protein name	Subcellular location	Molecular weight (kDa)	Intensity L	Intensity H	Ratio H/L[b]	Number of unique peptides[c]
P61604	10 kDa heat shock protein, mitochondrial	Mitochondrion matrix	10.932	53.54	185.32	1.52	2
P62158	Calmodulin	Cytoplasm, cytoskeleton	16.838	434.43	1380.96	1.40	7
P07355	Annexin A2	Basement membrane, extracellular matrix	38.604	89.47	250.96	1.23	6
P23528	Cofilin-1	Cell membrane, cell projection, cytoplasm, cytoskeleton, nucleus	18.502	88.9	236.91	1.17	3
P07737	Profilin-1	Cytoplasm, cytoskeleton	15.054	80.84	210.89	1.14	3
P10809	60 kDa heat shock protein, mitochondrial	Mitochondrion matrix	61.055	152.41	365.8	1.12	11
P14618	Pyruvate kinase PKM	Cytoplasm, nucleus	57.937	64.2	145.95	1.10	5
P21796	Voltage-dependent anion-selective channel protein 1	Mitochondrion outer membrane, cell membrane, membrane raft	30.773	47.39	117.57	1.09	2
P47756	F-actin-capping protein subunit beta	Cytoplasm, cytoskeleton	31.350	50.8	124.31	1.08	3
P04406	Glyceraldehyde-3-phosphate dehydrogenase	Cytoplasm, cytosol, cytoskeleton, nucleus, membrane	36.053	102.65	248.98	1.07	2
P06733	Alpha-enolase	Cytoplasm, membrane, nucleus	47.169	106.52	247.3	0.94	11
P08238	Heat shock protein HSP 90-beta	Cytoplasm	83.264	80.33	154.37	0.89	4
P63104	14-3-3 protein zeta/delta	Cytoplasm, melanosome	27.745	102.82	192.28	0.82	3
P61978	Heterogeneous nuclear ribonucleoprotein K	Cytoplasm, nucleus, cell projection	50.976	84.81	158.17	0.82	2
Q06830	Peroxiredoxin-1	Cytoplasm, melanosome	22.110	73.07	129.72	0.78	3
P68104	Elongation factor 1-alpha 1	Cytoplasm, nucleus	50.141	849.55	1293.57	0.65	23

TABLE 1 List of "heavy" labelled proteins interacting to HALT-1 in GST affinity purification (continue)

Accession number[a]	Protein name	Subcellular location	Molecular weight (kDa)	Intensity L	Intensity H	Ratio H/L[b]	Number of unique peptides[c]
P24534	Elongation factor 1-beta	Cytoplasm, cytosol	24.764	1460.27	1909.27	0.57	15
O43813	LanC-like protein 1	Cytoplasm,membrane	45.283	1420.34	1866.21	0.56	14
P26641	Elongation factor 1-gamma	Cytoplasm, cytosol, membrane, nucleus, extracellular exosome	50.119	1232.23	1538.48	0.55	19
Q9NS18	Glutaredoxin-2, mitochondrial	Mitochondrion, nucleus	18.052	254.9	196.13	0.34	2
Q03013	Glutathione S-transferase Mu 4	Cytoplasm, cytosol	25.561	150.83	108.36	0.32	2
P16152	Carbonyl reductase [NADPH] 1	Cytoplasm	30.375	3779.61	2653.005	0.29	79
P21266	Glutathione S-transferase Mu 3	Cytoplasm	26.560	5079.25	3246.36	0.27	51
P09488	Glutathione S-transferase Mu 1	Cytoplasm, cytosol	25.712	2459.63	1424.43	0.25	17
P09211	Glutathione S-transferase P	Cytoplasm, nucleus mitochondrion,	23.356	1888.39	672.05	0.17	31

[a] Accession number is the unique identifier assigned to the entire sequence record when the record is submitted to GenBank.

[b] Ratio of signal intensities of "heavy" and "light" sample pair are calculated by ProteinPilot with default setting to determine the relative level of protein in the two samples. It is calculated with the weighted average of log ratio of individual peptides belonging to the same protein after background subtraction.

[c] The number of distinct peptides that match to a single protein when MS/MS spectra is searched against a sequence database.

TABLE 2 List of "light" labelled proteins interacting to HALT-1 in GST affinity purification

Accession number[a]	Protein name	Subcellular localization	Molecular weight (kDa)	Intensity L	Intensity H	Ratio H/L[b]	Number of unique peptides[c]
P30050	60S ribosomal protein L12	Cytoplasm, cytosol, nucleus, nucleolus	17.819	1179.355	41.075	8.43	6
P15328	Folate receptor alpha	Cell membrane	29.819	1951.14	78.44	7.10	5
P05387	60S acidic ribosomal protein P2	Cytoplasm, cytosol, cell membrane	11.665	1108.02	50.19	6.30	5
P14923	Junction plakoglobin	Cell junction, cytoplasm, cell membrane	81.745	105.345	51.955	5.16	2
P60660	Myosin light polypeptide 6	Cytosol, cell membrane	16.930	19267.6	1136.03	4.84	12
P19338	Nucleolin	Nucleus, cytoplasm, cell membrane	76.614	743.97	59.785	3.54	6
Q96C19	EF-hand domain-containing protein D2	Membrane raft	26.697	423.78	82.84	1.46	4
P60709	Actin, cytoplasmic 1	Cytoplasm, cytoskeleton	41.737	3327.33	818.91	1.35	22
P52907	F-actin-capping protein subunit alpha-1	Cytoplasm, cytoskeleton	32.923	224.855	47.815	1.34	4
P38646	Stress-70 protein, mitochondrial	Mitochondrion, nucleus	73.680	260.65	56.87	1.31	2
P80723	Brain acid soluble protein 1	Cell membrane, cell projection	22.693	378.81	100.21	1.08	3
P07355	Annexin A2	Basement membrane, extracellular matrix	38.604	604.02	167.47	1.03	7
Q13813	Spectrin alpha chain, non-erythrocytic 1	Cytoplasm, cell cortex, cytoskeleton	284.539	287.7	83.165	0.94	2
Q09666	Neuroblast differentiation-associated protein AHNAK	Nucleus, cytoplasm, Cell membrane	629.101	393.555	40.63	0.86	3
P62258	14-3-3 protein epsilon	Cytoplasm, melanosome	29.174	264.94	119.03	0.64	2
P08238	Heat shock protein HSP 90-beta	Cytoplasm, melanosome	83.264	280.39	133.94	0.60	2
Q9BQE3	Tubulin alpha-1C chain	Cytoplasm, cytoskeleton, microtubule, nucleus	49.895	284.075	154.635	0.52	4
P10809	60 kDa heat shock protein, mitochondrial	Mitochondrion matrix	61.055	376.11	209.57	0.51	2

TABLE 2 List of "light" labelled proteins interacting to HALT-1 in GST affinity purification (continue)

Accession number[a]	Protein name	Subcellular localization	Molecular weight (kDa)	Intensity L	Intensity H	Ratio H/L[b]	Number of unique peptides[c]
Q06830	Peroxiredoxin-1	Cytoplasm, melanosome, nucleus, mitochondrion	22.110	136.1	76.53	0.51	2
P07737	Profilin-1	Cytoplasm, cytoskeleton	15.054	181.58	104.73	0.49	3
P21333	Filamin-A	Cytoplasm, cytoskeleton, cell cortex, cell membrane, nucleus	280.739	130.06	75.28	0.49	2
P07900	Heat shock protein HSP 90-alpha	Cytoplasm, melanosome, cell membrane, nucleus	84.660	190.47	110.995	0.492	2
P04075	Fructose-bisphosphate aldolase A	Cytoplasm, nucleus	39.420	228.03	138.29	0.47	3
P29401	Transketolase	Cytosol, nucleus	67.878	240.97	156.35	0.44	2
P68104	Elongation factor 1-alpha 1	Cytoplasm, nucleus;	50.185	1980.16	1423.34	0.40	19
P26641	Elongation factor 1-gamma	Nucleus, nucleolus, cytoplasm, cytosol, cell membrane	50.141	9287.73	7228.4	0.37	16
P24534	Elongation factor 1-beta	Cytoplasm, cytosol	24.764	1415.67	1199.09	0.34	9
O43813	LanC-like protein 1	Cytoplasm, cell membrane	45.283	3572.97	3836.755	0.27	10
P21266	Glutathione S-transferase Mu 3	Cytoplasm, nucleus	26.560	1546.04	1623.75	0.26	30
P16152	Carbonyl reductase [NADPH] 1	Cytoplasm	30.375	1221.59	1564.41	0.22	14
P09488	Glutathione S-transferase Mu 1	Cytoplasm	25.712	572.76	766.11	0.21	12
P09211	Glutathione S-transferase P	Cytoplasm, mitochondrion, nucleus, cell membrane	23.356	2163.21	4528.79	0.14	2

[a] Accession number is the unique identifier assigned to the entire sequence record when the record is submitted to GenBank.

[b] Ratio of signal intensities of "heavy" and "light" sample pair are calculated by ProteinPilot with default setting to determine the relative level of protein in the two samples. It is calculated with the weighted average of log ratio of individual peptides belonging to the same protein after background subtraction. The values of ratio H/L are inverted to keep consistency with the values presented in table 1.

[c] The number of distinct peptides that match to a single protein when MS/MS spectra is searched against a sequence database.

TABLE 3 Summary of putative HALT-1 interaction proteins after normalization

Accession number[a]	Gene name	Protein name	Normalized "heavy" SILAC ratio	Normalized "light" SILAC ratio	Significance level[b]
P30050	RPL12	60S ribosomal protein L12	100.00	8.42	3.22746E-04
P05387	RPLP2	60S acidic ribosomal protein P2	6.35	6.30	3.97908E-05
P15328	FOLR1	Folate receptor alpha	4.83	7.10	2.03048E-04
P19338	NCL	Nucleolin	5.20	3.54	8.075E-09

[a] Accession number is the unique identifier assigned to the entire sequence record when the record is submitted to GenBank.
[b] The statistical significant value shall be p-value < 0.05.

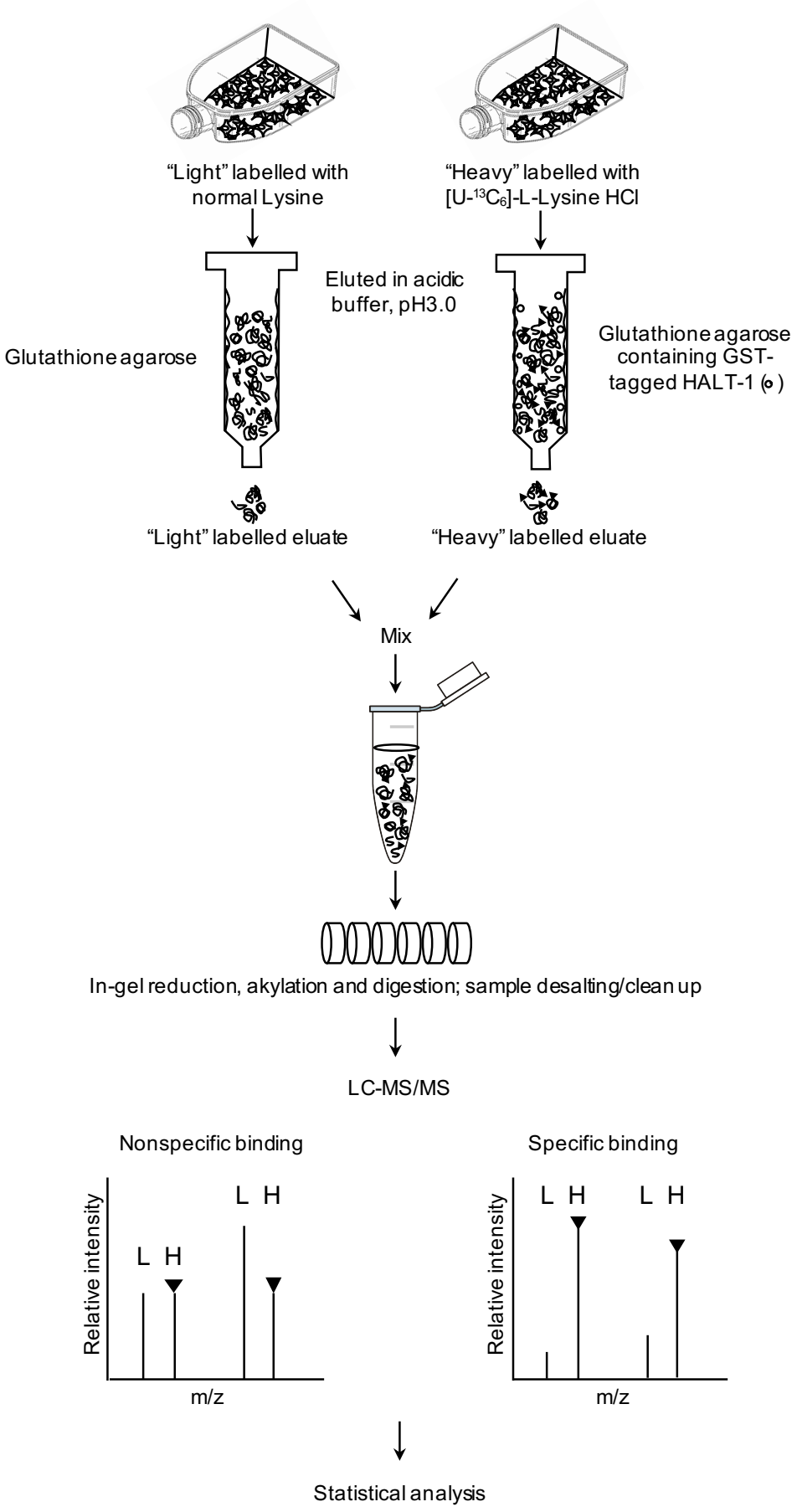
"Light" labelled with normal Lysine
"Heavy" labelled with [U-13C6]-L-Lysine HCl
Eluted in acidic buffer, pH3.0
Glutathione agarose
Glutathione agarose containing GST-tagged HALT-1 (o)
"Light" labelled eluate
"Heavy" labelled eluate
Mix
In-gel reduction, akylation and digestion; sample desalting/clean up
LC-MS/MS
Nonspecific binding
Specific binding
Relative intensity
L H
m/z
Statistical analysis

Figure 1

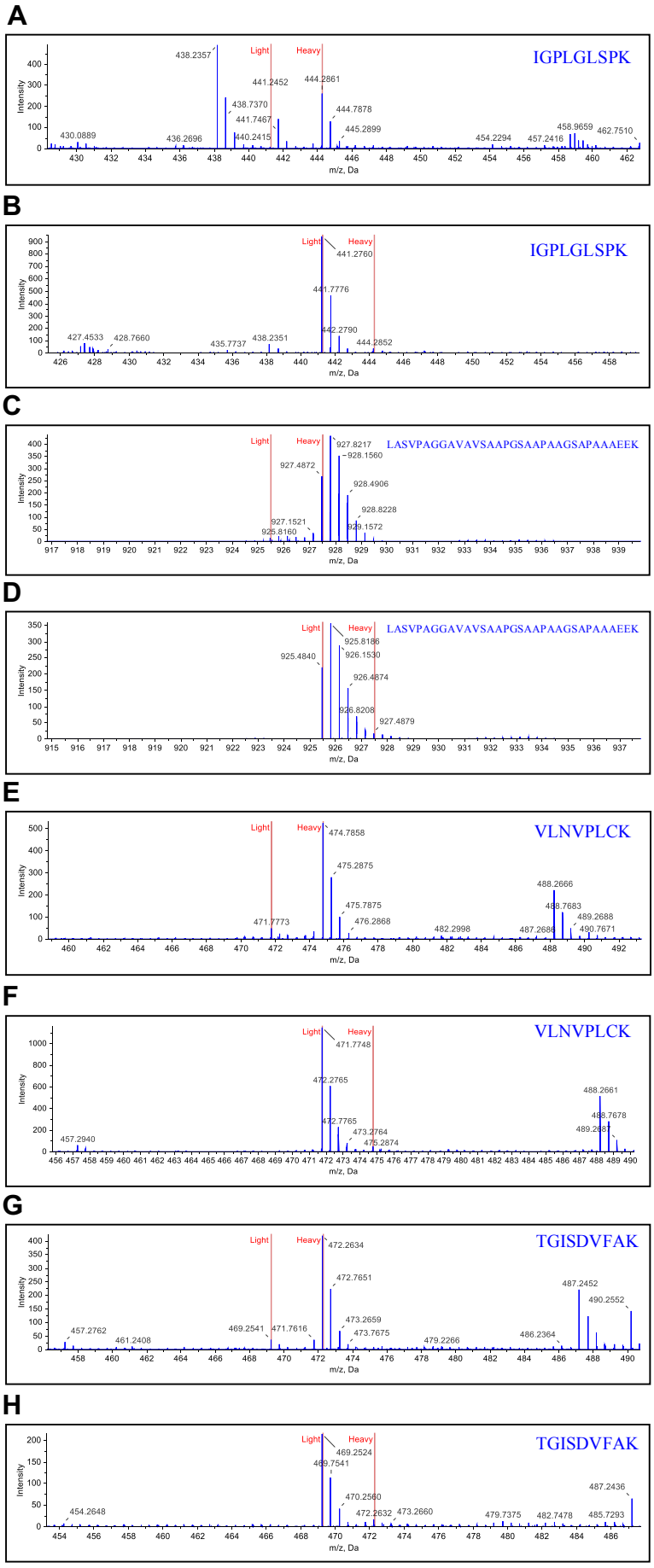
A
IGPLGLSPK
Light
Heavy
438.2357
441.2452
444.2861
438.7370
441.7467
440.2415
444.7878
445.2899
430.0889
436.2696
454.2294
457.2416
458.9659
462.7510
B
IGPLGLSPK
Light
Heavy
441.2760
441.7776
442.2790
427.4533
428.7660
435.7737
438.2351
444.2852
C
LASVPAGGAVAVSAAPGSAAPAAGSAPAAAEEK
Light
Heavy
927.8217
928.1560
927.4872
928.4906
928.8228
927.1521
925.8160
929.1572
D
LASVPAGGAVAVSAAPGSAAPAAGSAPAAAEEK
Light
Heavy
925.8186
925.4840
926.1530
926.4874
926.8208
927.4879
E
VLNVPLCK
Light
Heavy
474.7858
475.2875
488.2666
475.7875
488.7683
489.2688
471.7773
476.2868
482.2998
487.2686
490.7671
F
VLNVPLCK
Light
Heavy
471.7748
472.2765
488.2661
472.7765
488.7678
489.2687
457.2940
473.2764
475.2874
G
TGISDVFAK
Light
Heavy
472.2634
472.7651
487.2452
490.2552
457.2762
473.2659
469.2541
471.7616
473.7675
461.2408
479.2266
486.2364
H
TGISDVFAK
Light
Heavy
469.2524
469.7541
487.2436
470.2560
454.2648
472.2632
473.2660
479.7375
482.7478
485.7293
Intensity
m/z, Da

Figure 2

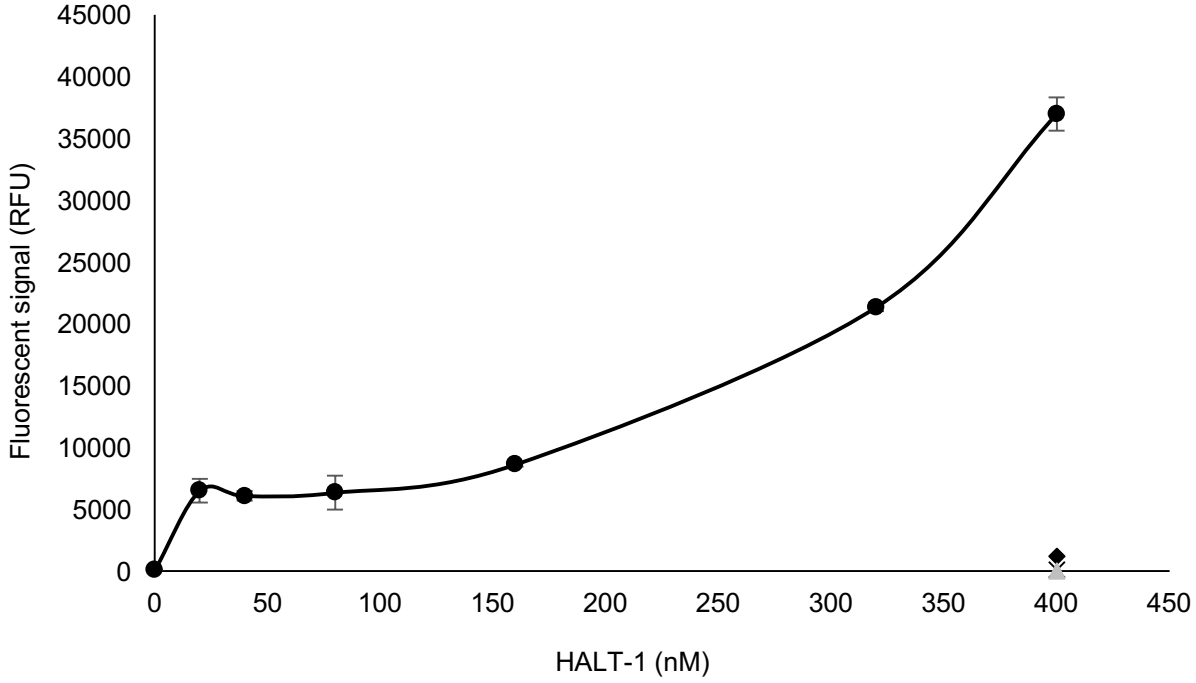
45000
40000
35000
30000
25000
20000
15000
10000
5000
0
Fluorescent signal (RFU)
0
50
100
150
200
250
300
350
400
450
HALT-1 (nM)

Figure 3

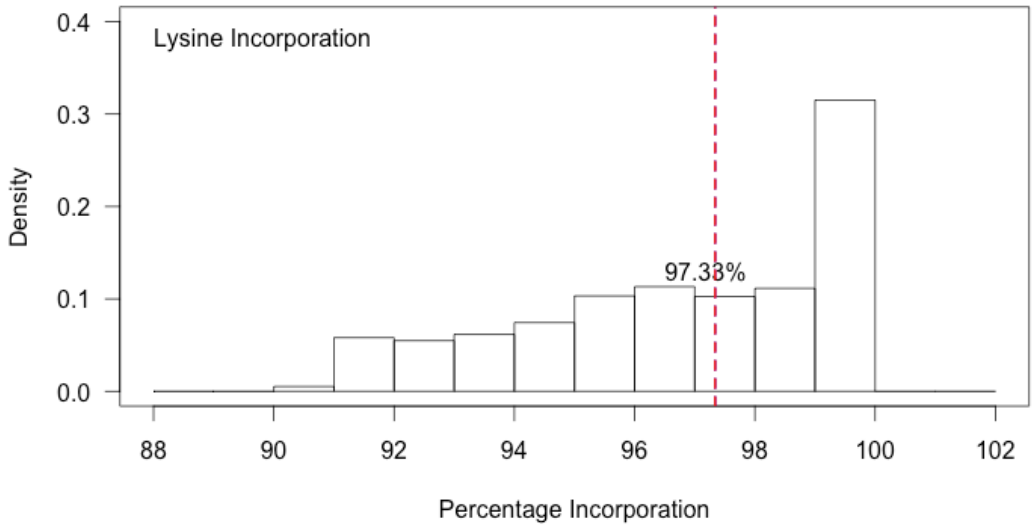

Supplementary Figure S1

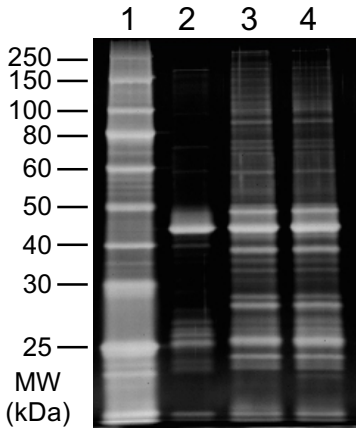

Supplementary Figure S2

Figure Legend

Fig. 1. Schematic workflow of GST affinity purification and SILAC-based quantitative mass spectrometry for identification of HALT-1 interacting partners. HeLa cells were grown in either "light" (L-Lysine HCl) or "heavy" ([U-$^{13}C_6$]-L-Lysine HCl) SILAC medium for 9 cell-doubling times. Whole cell lysate was subjected to GST affinity purification of which one column containing "light" labelled cell lysate with GST resin alone and the other column containing "heavy" labelled cell lysate with GST resin conjugated to GST-tagged (N-terminus) HALT-1. After washing, the bound proteins were independently eluted from both columns and then mixed equally before subjected to tube-gel digestion and LC-MS/MS based analysis. A low "light" MS ion peak together with an at least 2.0-fold higher "heavy" MS ion peak indicates as the putative protein interactor for HALT-1. For the second experiment, the procedure was performed in the same manner as described above except that the "light" labelled cell lysate and the "heavy" labelled cell lysate were reversed in the GST affinity purification.

Fig. 2. MS/MS spectra representing a SILAC unique peptide pair of RPL12, RPLP2, FOLR1 and NCL. Four HALT-1 interaction partners are unambiguously detected by LC-MS/MS and each putative protein has its "heavy" and "light" peptides appear on the same MS/MS spectrum. A and B, 60S ribosomal protein L12 (RPL12); C and D, 60S acidic ribosomal protein P2 (RPLP2); E and F, folate receptor alpha (FOLR1); G and H, nucleolin (NCL). A, C, E and G show the "heavy" peptides that are derived from the incubation with GST-tagged (N-terminus) HALT-1. Whereas, B, D, F and H show the "light" peptides that are derived from the incubation with GST-tagged (N-terminus) HALT-1. The ordinate indicates the relative intensity or abundance of peptides while the abscissa indicates the mass-to-charge ratio (m/z). Red vertical line indicates the position of "light" or "heavy" labelled pair of peptides in the spectrum. The sequence of SILAC peptide is shown on the right hand corner above the spectrum.

Fig. 3. Immobilized FOLR-1 ELISA. Data demonstrated the specific binding of FOLR-1 by *Hydra* HALT-1. The mean of fluorescent signal for triplicate experiments was measured with various concentrations of HALT-1. Standard deviation was calculated from the triplicate results and indicated by the upper and lower error bars at each data point. Control without either FOLR-1 (◆), anti-HALT-1 antibody (▲) or goat anti-rabbit IgG (X) was carried out at the highest concentration of HALT-1 (400 nM or 10 µg/mL).

Supplementary Figure Legend

Supplementary Fig. S1. SILAC incorporation in HeLa cells after 9 doubling times. Vertical dashed line indicates the percentage of SILAC labelling efficiency (97.33%). X-axis represents the incorporation levels of SILAC amino acid, "heavy" ([U-$^{13}C_6$]-L-Lysine HCl); and y-axis represents the probability of peptides that were coupled with SILAC amino acid.

Supplementary Fig. S2. Electrophoretic analysis of the pool of eluate fractions after GST affinity purification. Lane 1, unstained protein ladder with broad range 10-250 kDa; lane 2, purified recombinant GST-tagged HALT-1 (2.5 µg); lane 3, the pool of "light" and "heavy" labelled eluates in which "heavy" labelled lysate has been incubated with GST-tagged (N-terminus) HALT-1; lane 4, the pool of "light" and "heavy" labelled eluates in which "light" labelled lysate has been incubated with GST-tagged (N-terminus) HALT-1. The expected size of GST-tagged HALT-1 was approximately 45.8 kDa.